Diffractive production of vector mesons at HERA

B. Waugh[a*]
for the H1 and ZEUS collaborations

[a]Dept. of Physics and Astronomy, University of Manchester, Oxford Road, Manchester M13 9PL, UK.

Selected recent results on diffractive vector-meson production from the H1 and ZEUS experiments at the HERA *ep* collider are reviewed and compared with the predictions of the vector-meson dominance model and of perturbative QCD. The helicity structure and energy dependence are studied for production of light and heavy vector mesons across a range of the photon virtuality Q^2 and the squared four-momentum transfer t. The cross section for elastic photoproduction of Υ is also presented.

1. INTRODUCTION

The HERA experiments H1 and ZEUS have greatly extended the kinematic range covered by fixed-target experiments, enabling more detailed studies of diffractive vector-meson production both in the completely soft regime and in the cases where one or more of the involved scales are large enough for perturbative QCD to be applied. The relevant scales are: Q^2, the virtuality of the incident photon; t, the squared four-momentum exchange at the proton vertex; and M_V, the mass of the produced vector meson.

The diffractive photo- and electroproduction of vector mesons, $\gamma^{(*)}p \to VX$, may be divided into the *elastic* process, where X is a proton, and the *proton dissociation* process, where X is a different low-mass hadronic state.

1.1. Regge theory and the vector-meson dominance model

Elastic photoproduction ($Q^2 \approx 0$) of light vector mesons at low $|t|$, where there is no hard scale and perturbative QCD therefore cannot be applied, is well described by an approach combining the vector-meson dominance model (VDM) with Regge theory, illustrated in figure 1(a). The wave function of the photon includes contributions from off-shell hadronic states, in particular the vector mesons, which have the same quantum numbers ($J^{PC} = 1^{--}$) as the photon. The interaction between the proton and this hadronic component of the photon is modelled by the exchange of Regge trajectories.

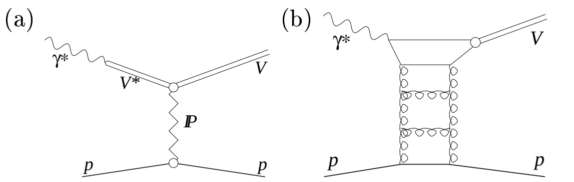

Figure 1. Elastic vector-meson production $\gamma^{(*)}p \to Vp$: (a) as exchange of a pomeron ($I\!P$) in the VDM-Regge picture and (b) as exchange of a gluon ladder in perturbative QCD.

At high γp centre-of-mass energies W, the process is dominated by pomeron exchange. The cross section grows slowly with W, corresponding to a small value of the pomeron intercept α_0, as also seen in hadron-hadron scattering [1]. The distribution of t, the squared four-momentum transfer, peaks near zero and falls off approximately exponentially $\sim e^{-b|t|}$. The helicity of the incoming photon is retained by the outgoing vector meson; this is referred to as "s-channel helicity conservation" (SCHC).

*Current address: DESY (FH1T), Notkestraße 85, 22607 Hamburg, Germany

1.2. Perturbative QCD

For perturbative QCD to be applied, there must be a hard scale (Q^2, t or M_V) in the process to be described. Diffractive production of a vector meson corresponds in QCD to the exchange of a pair or ladder of gluons carrying no net colour, as illustrated in figure 1(b). The cross section is thus related to the density of gluons in the proton. As the energy W is increased, the corresponding momentum fraction $x_{g/p}$ decreases, resulting in a rapid increase of the cross section with energy, related to the rise in the gluon density at low x. SCHC does not necessarily apply in perturbative QCD models.

2. HELICITY

The contributions of different helicity states to the cross section are given by the helicity amplitudes $T_{\lambda_V \lambda_{\gamma^*}}$, where the indices λ_V and λ_{γ^*} are the helicities of the outgoing vector meson and the incoming virtual photon respectively. These amplitudes are related to the spin-density matrix elements r^{α}_{ij}, which can be determined from the distributions of three angles: θ and φ, the polar and azimuthal angles of the decay products in the rest frame of the vector meson; and ϕ, the angle between the electron scattering plane and the vector-meson production plane, defined in the $\gamma^{(*)}p$ centre-of-mass frame.

These measurements provide a way of testing the validity of SCHC, since several of the helicity amplitudes, and hence several of the matrix elements, must be zero if SCHC is obeyed. Fifteen of the spin-density matrix elements can be measured in the scattering of unpolarized electron and proton beams, as performed at HERA.

2.1. Helicity in ρ electroproduction

Figure 2 shows the spin-density matrix elements measured by H1 and ZEUS in ρ electroproduction ($Q^2 > 2.5\,\mathrm{GeV}^2$). Predictions from SCHC are shown, as well as the predictions of a model using perturbative QCD. Most of the matrix elements constrained by SCHC are close to the predicted values, but r^5_{00} shows a significant deviation from zero, representing a small violation of SCHC. This matrix element is approximately proportional to the amplitude for the helicity-flip process in which a transversely polarized photon produces a longitudinally polarized vector meson. The ratio of this helicity-flip amplitude to the amplitude for the helicity-conserving process is calculated from the H1 measurement to be $(8 \pm 3)\%$. The perturbative QCD model does not deviate much from SCHC in most of the matrix elements, but it improves on the SCHC predictions in that it is compatible with the helicity-flip contribution represented by the non-zero value of r^5_{00}.

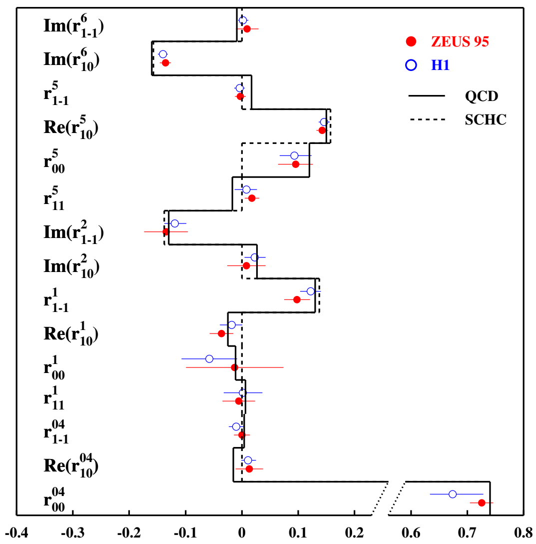

Figure 2. Spin-density matrix elements measured for elastic electroproduction of ρ mesons [2,3]. The predictions of SCHC and of a perturbative QCD model [4] are also shown.

The matrix element r^{04}_{00} measures the fraction of produced vector mesons which are longitudinally polarized. If SCHC is assumed to hold, the ratio of the cross sections for elastic production of vector mesons by longitudinal and transverse photons can be calculated using the approximation $R = \frac{\sigma_L}{\sigma_T} \simeq \frac{1}{\epsilon} \cdot \frac{r^{04}_{00}}{1-r^{04}_{00}}$, where ϵ is the ratio of the fluxes of longitudinally and transversely polarized photons and is close to unity in the kinematic range covered here. The small violation of SCHC discussed above does not significantly affect the results, which are shown in figure 3. The shape of the Q^2 dependence is reasonably well described by several models based on perturbative QCD (Royen-Cudell [5], Martin-Ryskin-Teubner [6]) or on the generalized VDM (Schildknecht-Schuler-Surrow [7]).

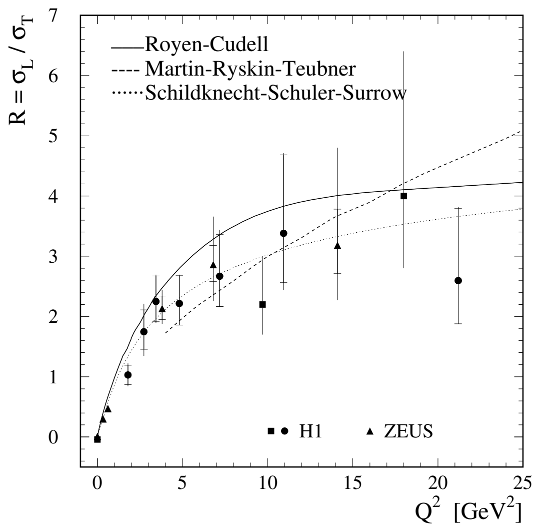

Figure 3. Ratio of longitudinal to transverse cross section for elastic electroproduction of ρ mesons, plotted against Q^2 [3]. The curves are the predictions of different models (see text).

2.2. Helicity in ρ photoproduction at large $|t|$

The helicity structure of diffractive ρ production has also been studied by ZEUS in photoproduction ($Q^2 \approx 0$) at large values of $|t|$, from $1\,\mathrm{GeV}^2$ up to about $6\,\mathrm{GeV}^2$. In this range, the process is dominated by proton-dissociation events. Here the photon virtuality Q^2 no longer provides a hard scale for perturbative calculations, but an interesting question is whether $|t|$ can fill this role, and how large it must be for perturbative QCD to be valid.

It has been predicted that a signature of the fully perturbative region is the dominance of longitudinally polarized vector mesons [8]. This would be observed as a large value of the matrix element r^{04}_{00}, which is shown for several values of $|t|$ in figure 4(a). It is seen that longitudinal polarization does not in fact dominate at the values of $|t|$ reached here, meaning that the fully perturbative region has not been reached at $|t| \approx 5\,\mathrm{GeV}^2$.

Figure 4(b) shows the matrix element r^{04}_{1-1} as a function of $|t|$. This quantity is sensitive to the double-flip contribution, in which a transversely polarized photon produces a vector meson with the opposite helicity. The non-zero value of r^{04}_{1-1} measured at large values of $|t|$ demonstrates that SCHC is violated in this region.

3. ENERGY DEPENDENCE

Figure 5 shows the cross sections for elastic electroproduction of ρ and ϕ mesons plotted against W for a number of different values of Q^2. The energy dependence is well described by a power law $\sigma \propto W^\delta$, and the steepness of the slope, δ, can be plotted against Q^2, as shown in figure 6, to look for evidence of perturbative effects as Q^2 is increased. There is clear evidence that the energy dependence is indeed steeper at high Q^2 than in photoproduction, where $\delta \approx 0.2$, although the shape of the curve is not well constrained at the present level of accuracy.

In kinematic regions where perturbative QCD is valid, the elastic production of vector mesons is sensitive to the gluon content of the proton, and can be used to measure the gluon distribution. Figure 7 shows the forward longitudinal cross section for elastic ρ electroproduction as a function of the fraction, x, of the momentum of the proton entering the process. The results are compared with the predictions of a perturbative QCD model using various parameterizations of the parton densities in the proton. The sensitivity of this process to the parton content of the proton is clear.

Figure 8 shows the energy dependence of elas-

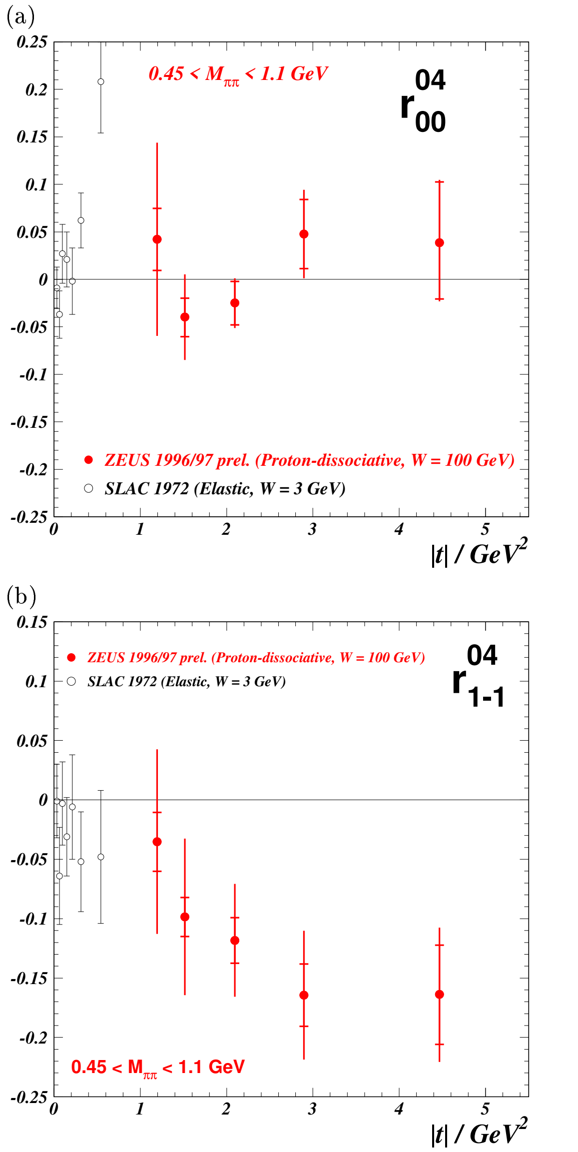

Figure 4. The matrix elements (a) r_{00}^{04} and (b) r_{1-1}^{04}, plotted against $|t|$ for diffractive photoproduction of ρ mesons [9].

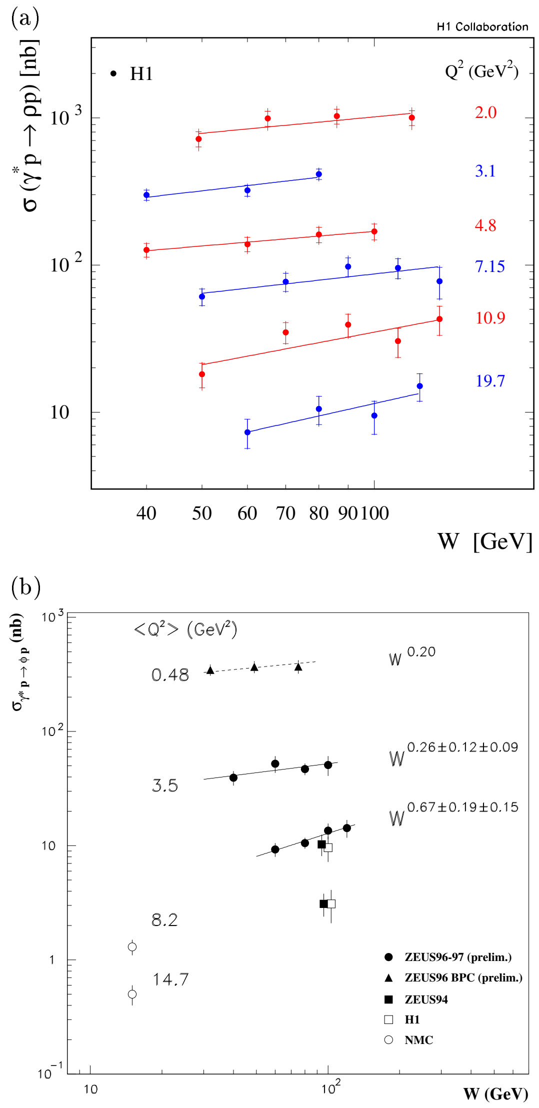

Figure 5. Energy dependence of the cross section for elastic electroproduction of (a) ρ mesons [3] and (b) ϕ mesons [10].

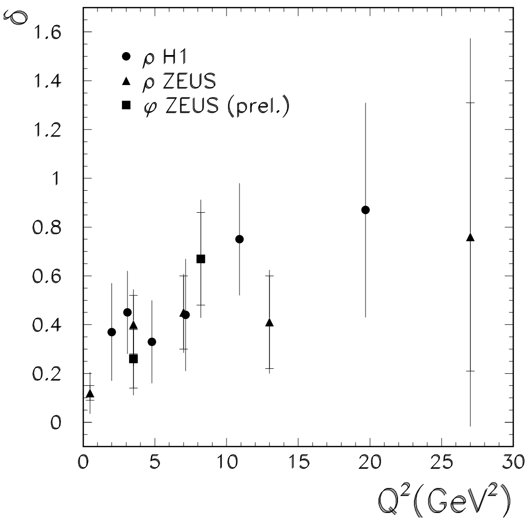

Figure 6. Slope of energy dependence for elastic production of vector mesons plotted against Q^2 [3,11].

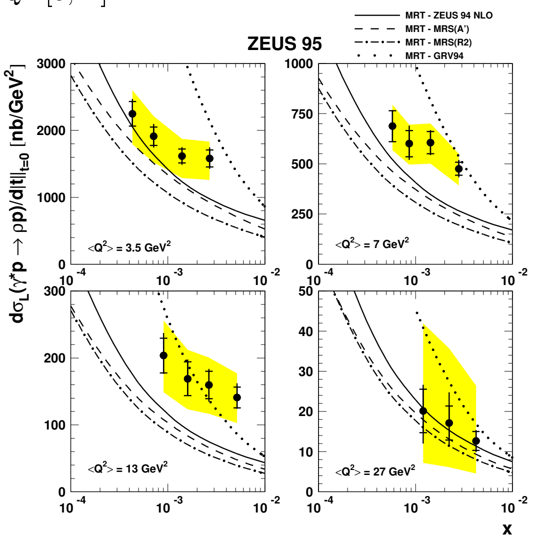

Figure 7. Forward longitudinal cross section for elastic production of ρ mesons plotted against the momentum fraction x [11]. Also shown are the predictions of a perturbative QCD model [12], illustrating the sensitivity of this quantity to the gluon content in the proton.

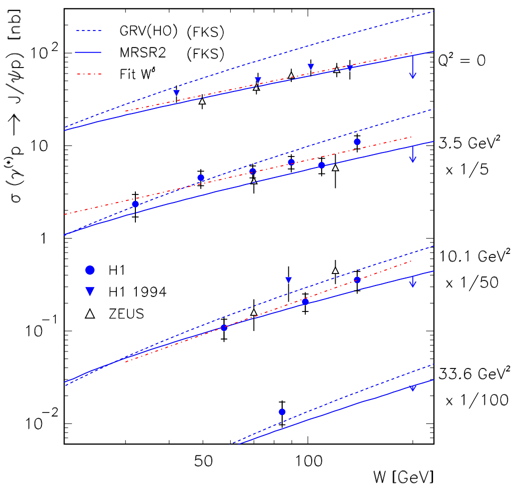

Figure 8. Energy dependence of the cross section for elastic electroproduction of J/ψ mesons [11, 13]. Also shown are the predictions of a perturbative QCD model [14]. The downward arrows on the curves show the effect of varying the charm mass from 1.4 to 1.5 GeV.

tic production of J/ψ mesons for different values of Q^2. Even in photoproduction, the energy dependence is significantly steeper than it is for the lighter vector mesons, indicating the importance of the vector-meson mass as a hard scale for perturbative QCD. As the second scale, Q^2, is increased, there is no significant further increase in the slope above that in photoproduction. The sensitivity of this process to the gluon density in the proton is illustrated by the predictions, also shown, of a perturbative QCD model using different parton densities. In the J/ψ case the results are also dependent on the value assumed for the mass of the charm quark, as indicated by the arrows in the figure.

4. Υ PHOTOPRODUCTION

The cross section for elastic photoproduction of the $\Upsilon(1S-3S)$ mesons, with masses $\sim 10\,\mathrm{GeV}$, has also been measured. Using an assumption for the relative contributions of the different states, which are not resolved by the mass resolution of the detectors, the cross section for $\Upsilon(1S)$ production is extracted. The results are shown in figure 9. The present level of precision does not

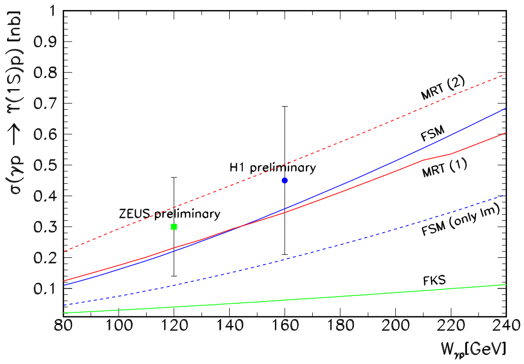

Figure 9. Cross sections for the elastic photoproduction of Υ mesons [15]. The curves show the predictions of QCD calculations with (FSM, MRT [16,17]) and without (FKS [14]) off-diagonal parton distributions.

allow the energy dependence to be measured. At large vector-meson masses the two gluons forming the "uprights" of the exchanged gluon ladder have very different momenta. This means that the cross section is only well described if the off-diagonal gluon distribution $x'g(x,x')$ is used. Calculations made neglecting this contribution fall below the data.

5. CONCLUSIONS

As the various scales involved in diffractive vector-meson production (Q^2, $|t|$ and m_V) are increased, perturbative QCD starts to be applicable, taking over from the VDM-Regge approach which is successful in the soft region.

Production of J/ψ shows characteristics of a hard process even at $Q^2 \approx 0$, while ρ production shows signs of deviation from soft behaviour as Q^2 is increased. Measurements of ρ photoproduction show that this process is not yet fully perturbative at $|t|$ of $\sim 5\,\mathrm{GeV}^2$. Discovering the value of each scale at which the fully perturbative regime is entered, as well as elucidating the characteristics of the transition region, will require further measurements with higher precision.

Within perturbative QCD, measurements of diffractive vector-meson production are sensitive to the gluon content of the proton. The cross section for Υ photoproduction proves the importance of off-diagonal parton distributions for large vector-meson masses.

REFERENCES

1. A. Donnachie and P. V. Landshoff, Phys. Lett. B296 (1992) 227.
2. A. Savin, talk at DIS 99, Zeuthen, April 1999.
3. H1 Collab., DESY 99–010, submitted to Eur. Phys. J. C.
4. D. Yu. Ivanov and R. Kirschner, Phys. Rev. D58 (1998) 114026.
5. I. Royen and J.-R. Cudell, Nucl. Phys. B545 (1999) 505.
6. A. D. Martin, M. G. Ryskin and T. Teubner, Phys. Rev. D55 (1997) 4329.
7. D. Schildknecht, G. A. Schuler and B. Surrow, Phys. Lett. B449 (1999) 328.
8. I. F. Ginzburg and D. Yu. Ivanov, Phys. Rev. D54 (1996) 5523;
   S. J. Brodsky, M. Diehl, P. Hoyer and S. Peigné, Phys. Lett. B449 (1999) 306.
9. J. Crittenden, talk at DIS 99, Zeuthen, April 1999.
10. ZEUS Collab., Paper 793 submitted to ICHEP 98, Vancouver, July 1998.
11. ZEUS Collab., Eur. Phys. J. C6 (1999) 603.
12. L. Frankfurt, W. Koepf and M. Strikman, Phys. Rev. D54 (1996) 3194.
13. H1 Collab., DESY 99–026, submitted to Eur. Phys. J. C.
14. L. Frankfurt, W. Koepf and M. Strikman, Phys. Rev. D57 (1998) 512.
15. ZEUS Collab., Phys. Lett. B437 (1998) 342;
    H1 Collab., Paper 574 submitted to ICHEP 98, Vancouver, July 1998.
16. L. Frankfurt, M. F. McDermott and M. Strikman, JHEP 02 (1999) 002.
17. A. D. Martin, M. G. Ryskin and T. Teubner, Phys. Lett. B454 (1999) 339.